Dalton Transactions

PAPER

View Article Online
View Journal

Cite this: DOI: 10.1039/c8dt02290a

Heterometallic $Cu^{II}Fe^{III}$ and $Cu^{II}Mn^{III}$ alkoxo-bridged complexes revealing a rare hexanuclear $M_6(\mu\text{-}X)_7(\mu_3\text{-}X)_2$ molecular core†

Oksana V. Nesterova, *[a] Dmytro S. Nesterov, *[a] Beáta Vranovičová,[b] Roman Boča[b] and Armando J. L. Pombeiro *[a]

The novel hexanuclear complexes $[Cu_4Fe_2(OH)(Piv)_4(t\text{BuDea})_4Cl]\cdot 0.5CH_3CN$ (**1**) and $[Cu_4Mn_2(OH)(Piv)_4(t\text{BuDea})_4Cl]$ (**2**) were prepared through one-pot self-assembly reactions of copper powder and iron(II) or manganese(II) chloride with *N*-*tert*-butyldiethanolamine (H_2tBuDea) and pivalic acid (HPiv) in acetonitrile. Crystallographic studies revealed the uncommon molecular core type $M_6(\mu\text{-}X)_7(\mu_3\text{-}X)_2$ in **1** and **2**, which can be viewed as a combination of two trimetallic $M_3(\mu\text{-}X)_2(\mu_3\text{-}X)$ fragments joined by three bridging atoms. The analysis and classification of the hexanuclear complexes having a $M_3(\mu\text{-}X)_2(\mu_3\text{-}X)$ moiety as a core forming fragment using data from the Cambridge Structural Database (CSD) were performed. Variable-temperature (1.8–300 K) magnetic susceptibility measurements of **1** showed a decrease of the effective magnetic moment value at low temperature, indicative of antiferromagnetic coupling between the magnetic centres ($J_{Fe-Cu}/hc = -6.9$ cm^{-1}, $J_{Cu-Cu}/hc = -4.1$ cm^{-1}, $J_{Fe-Fe}/hc = -24.2$ cm^{-1}). Complex **1** acts as a catalyst in the reaction of mild oxidation of cyclohexane with H_2O_2, showing the yields of products, cyclohexanol and cyclohexanone, up to 17% using pyrazinecarboxylic acid as a promoter. In the oxidation of *cis*-1,2-dimethylcyclohexane with *m*-chloroperoxybenzoic acid (*m*-CPBA), 70% of retention of stereoconfiguration was observed for tertiary alcohols. Compound **1** also catalyses the amidation of cyclohexane with benzamide. In all three catalytic reactions the by-products were investigated in detail and discussed.

Received 4th June 2018,
Accepted 10th July 2018

DOI: 10.1039/c8dt02290a

rsc.li/dalton

Introduction

The search towards novel molecule-based materials, able to combine useful physico-chemical properties, such as magnetism and catalysis, has led to particular interest in polynuclear coordination compounds.[1] Apart from other possibilities, their multifunctionality can be realized by the involvement of two or more dissimilar metal atoms into the final close-packed molecule. Poly- and high-nuclear heterometallic coordination compounds[1a,2] represent a class of materials with recognized magnetic[3] and catalytic[1a,4] effects, appearing from synergic interactions of a few different metals within one complex molecule. In pursuit of our research on heterometallic high-nuclear coordination compounds, we applied the "direct synthesis" approach,[2] which is based on the spontaneous self-assembly and allows the use of metal powder(s) as the starting material and simple flexible ligands, such as aliphatic aminoalcohols.[1a,5] In this way, the formation of a complex high-nuclear structure proceeds in a single-pot, easy and "straightforward" method avoiding the separate steps of building block construction. Using this synthetic strategy a series of heterometallic complexes of various nuclearities were obtained.[1a,2] Many of them show rather rare or even unique types of molecular structure cores and, moreover, can reveal a high catalytic activity in the oxidation of alkanes with peroxides under mild conditions[1a,6] and an interesting magnetic behaviour.[7]

It has been shown that the simultaneous use of aminoalcohols and carboxylate ligands having bulky substituents (such as *tert*-butyl groups) may lead to unexpected ligand coordination modes[8] and polynuclear structures.[9] In the present study, we were interested to combine the "direct synthesis"

[a]*Centro de Química Estrutural, Complexo I, Instituto Superior Técnico, Universidade de Lisboa, Avenida Rovisco Pais, 1049-001 Lisboa, Portugal. E-mail: pombeiro@tecnico.ulisboa.pt, dmytro.nesterov@tecnico.ulisboa.pt, oksana.nesterova@tecnico.ulisboa.pt*

[b]*Department of Chemistry, FPV, University of SS Cyril and Methodius, 917 01 Trnava, Slovakia*

†Electronic supplementary information (ESI) available: Selected geometrical parameters (distances/Å and angles/°) for **1** and **2**. The analysis of the $\{M_6(\mu\text{-}X)_7(\mu_3\text{-}X)_2\}$ Molecular Structure Type (MST). Figures (plots, chromatograms and mass spectra). Details of ^{18}O incorporation analysis; chromatograms of reaction products for cyclohexane and *cis*-1,2-dimethylcyclohexane (*cis*-1,2-DMCH) oxidation; accumulations of products for oxidation of *cis*-1,2-DMCH and $[\mathbf{1}]_0 = 4.1 \times 10^{-4}$ M; EI mass spectra of normal and ^{18}O-labeled products. CCDC 1447617 1816439. For ESI and crystallographic data in CIF or other electronic format see DOI: 10.1039/c8dt02290a

synthetic approach with the aminoalcohol/carboxylic acid ligand system, expecting that both these powerful approaches would lead to novel polynuclear assemblies.

A potential feature of the coordination compounds bearing bulky hydrophobic groups (such as *tert*-butyl ones) is their solubility in low-polar solvents, such as benzene or aliphatic hydrocarbons. This property is important for the studies of homogeneous catalytic processes typically proceeding in such solvents. As heterometallic complexes, particularly those involving copper, manganese or iron, were shown as active catalysts in the reactions of alkane C–H functionalization,[1a,4,10] hence we aimed at the preparation of polynuclear heterometallic compounds based on these metals with bulky N,O-donor ligands and the investigation of their catalytic activity in valuable C–H activation processes,[11] such as hydroxylation[1a,10a] and amidation[12] of cycloalkanes and their derivatives in the presence of peroxide oxidants.

In the present work, we have studied the interaction of copper powder and iron(II) or manganese(II) chlorides with *N-tert*-butyldiethanolamine (H_2*t*BuDea) and pivalic acid (HPiv) that afforded the novel heterometallic complexes $[Cu_4Fe_2(OH)(Piv)_4(tBuDea)_4Cl]\cdot 0.5CH_3CN$ (**1**) and $[Cu_4Mn_2(OH)(Piv)_4(tBuDea)_4Cl]$ (**2**). The magnetic and alkane oxidation catalytic properties of **1** are discussed herein.

Experimental section

General

All chemicals were of reagent grade and used as received. All experiments were carried out in air. Elemental analyses for C, H and N were carried out by the Microanalytical Service of the Instituto Superior Técnico. Infrared spectra (4000–400 cm^{-1}) were recorded on a Vertex 70 (Bruker) instrument in KBr pellets. Mass spectra were obtained using an LCQ Fleet mass spectrometer with an ESI source (Thermo Scientific). Powder X-ray data were collected at room temperature using a Bruker D8 Advance diffractometer.

Synthesis of $[Cu_4Fe_2(OH)(Piv)_4(tBuDea)_4Cl]\cdot 0.5CH_3CN$ (1)

Copper powder (0.16 g, 2.5 mmol), $FeCl_2\cdot 4H_2O$ (0.99 g, 5 mmol), pivalic acid (0.26 g, 2.5 mmol), *N-tert*-butyldiethanolamine (2.4 g, 15 mmol) and triethylamine (0.7 mL, 5 mmol) were dissolved in CH_3CN (30 mL) and magnetically stirred at 50–60 °C (2 h). The resulting dark-brown solution was filtered off twice and dark-brown crystals suitable for X-ray crystallographic study were formed within four days. Yield: 0.58 g (63% based on copper). Anal. calc. for $C_{53}H_{106.50}ClCu_4Fe_2N_{4.50}O_{17}$ (M = 1480.23): C, 43.00; N, 4.26; H, 7.25%. Found: C, 42.9; N, 4.5; H, 7.3%. The compound is sparingly soluble in DMSO, DMF and insoluble in water.

Synthesis of $[Cu_4Mn_2(OH)(Piv)_4(tBuDea)_4Cl]$ (2)

Copper powder (0.16 g, 2.5 mmol), $MnCl_2\cdot 4H_2O$ (0.99 g, 5 mmol), pivalic acid (0.26 g, 2.5 mmol), *N-tert*-butyldiethanolamine (2.4 g, 15 mmol) and triethylamine (0.7 mL, 5 mmol) were dissolved in CH_3CN (30 mL) and magnetically stirred at 50–60 °C (5 h). The resulting dark-brown solution was filtered off and left untouched for 1 month for standing at r.t. After this, ^{i}PrOH was added in small portions the next month, which afforded an oily substance with the inclusion of a small amount of dark-brown crystals suitable for X-ray crystallographic study. The crystals were carefully removed from the oil, washed with methanol and dried. Anal. calc. for $C_{52}H_{105}ClCu_4Mn_2N_4O_{17}$ (M = 1457.88): C, 42.84; N, 3.84; H, 7.27%. Found: C, 43.0; N, 4.2; H, 7.4%.

Crystallography

Crystal data for 1. $C_{53}H_{106.50}ClCu_4Fe_2N_{4.50}O_{17}$, M = 1480.23, a = 16.296(3) Å, b = 23.480(5) Å, c = 36.268(8) Å, β = 99.460(8)°, V = 13 688(5) Å^3, T = 150(2) K, space group $C2/c$, Z = 8, MoKα, 102 878 reflections measured, 14 044 independent reflections (R_{int} = 0.1117). The final R_1 values were 0.0435 ($I > 2\sigma(I)$). The final w$R(F^2)$ values were 0.0975 (all data). The goodness of fit on F^2 was 1.018.

Crystal data for 2. $C_{52}H_{105}ClCu_4Mn_2N_4O_{17}$, M = 1457.88, a = 22.8621(15) Å, b = 16.6480(15) Å, c = 19.7908(16) Å, β = 114.979(6)°, V = 6828.0(10) Å^3, T = 150(2) K, space group Cc, Z = 4, MoKα, 51 971 reflections measured, 14 023 independent reflections (R_{int} = 0.1286). The final R_1 values were 0.0634 ($I > 2\sigma(I)$). The final w$R(F^2)$ values were 0.1339 (all data). The goodness of fit on F^2 was 0.996.

The X-ray diffraction data for complexes **1** and **2** were collected using a Bruker AXS KAPPA APEX II diffractometer with graphite monochromated Mo-Kα radiation. Cell parameters were retrieved using Bruker SMART and refined using Bruker SAINT[13] on all the observed reflections. Absorption corrections were applied using SADABS.[14] The structure was solved by direct methods and refined against F^2 using the program SHELXL-2016/6.[15] The structure of **2** was refined as an inversion twin with 4.8% of the inverted component, leading to a Flack parameter of 0.05(2).

The *tert*-Bu groups C44–C47 in both **1** and **2** were modelled as being disordered over two positions, having A and B atom labels, with populations 0.553(11) and 0.447(11) for **1**, and 0.51(4) and 0.49(4) for **2**, respectively. The atoms of the disordered *tert*-Bu groups were refined with isotropic displacement parameters. The chlorine atom Cl1 in **2** was found to be disordered over two positions, Cl1A and Cl1B, with occupancies 0.324(9) and 0.676(9), respectively. The presence of a difference peak of 0.96 e Å^{-3} in the Fourier map around the ClB atom suggested the possibility of the presence of other atoms, presumably water molecules, which coordinate with Cu2. However, attempts to treat this peak as disordered water were unsuccessful with unacceptable thermal parameters. Furthermore, the presence of such water molecules would result in a too short ClA–O(water) distance of less than 2 Å. Hence this weak difference peak was ignored.

The H1 hydrogen atoms of the coordinated OH group in **1** and **2** were located in difference Fourier maps and refined using a riding model using U_{iso} = 1.5U_{eq} (for **1**) or refined freely (for **2**). All other hydrogen atoms were placed at calcu-

lated positions and refined the same model with $U_{iso} = nU_{eq}$ (n = 1.5 for H atoms of the methyl group and water H atoms, and n = 1.2 for other H atoms).

Crystallographic data for the reported structures can be obtained by quoting the deposition numbers CCDC 1447617 (**1**) and 1816439 (**2**).†

Magnetic measurements

The magnetic data for **1** were obtained for a polycrystalline sample with a SQUID magnetometer (MPMS-XL7, Quantum Design) in the RSO mode of detection.

Gas chromatography and mass spectrometry

A PerkinElmer Clarus 500 gas chromatograph, equipped with a polar capillary column (SGE BP-20; 30 m × 0.32 mm × 25 μm) and a FID detector, was used for analyses of the reaction products of cyclohexane oxidation. The following GC conditions were used: 100 °C (1 min), 100–160 °C (10 degrees per minute), 160 °C (1 min), 8 min total run time; 200 °C injector temperature. A PerkinElmer Clarus 600 gas chromatograph, equipped with two non-polar capillary columns (SGE BPX5; 30 m × 0.32 mm × 25 μm), one having an EI-MS (electron impact) quadrupole detector and the other one with a FID detector, was used for other analyses of the reaction mixtures. The following GC conditions were used: 50 °C (3 min), 50–120 °C (8 degrees per minute), 120–300 °C (35 degrees per minute), 300 °C (3.11 min), 20 min total run time; 200 °C injector temperature. For analysis of cyclohexane amidation products a different program was employed: 50 °C (3 min), 50–150 °C (30 degrees per minute), 150–300 °C (14 degrees per minute), 300 °C (2.95 min), 20 min total run time; 200 °C injector temperature. Helium was used as the carrier gas (constant 14 psi pressure and constant 1 mL min^{-1} flow for Clarus 500 and Clarus 600 devices, respectively). All EI mass spectra were recorded with 70 eV energy. The $^{16}O/^{18}O$ compositions of the oxygenated products were determined by the relative abundances of mass peaks at $m/z = M^+/(M^+ + 2)$ molecular ion peaks. Estimation of low-level ^{18}O incorporations into tertiary *trans*- and *cis*-alcohols required a special correction to exclude the systematic errors of the mass spectrometer (see the ESI†).

Catalytic oxidation of alkanes

The reactions were typically carried out in air in thermostated cylindrical vials with vigorous stirring. Firstly, CH_3CN and CH_3NO_2 (GC internal standard, final $[CH_3NO_2]$ = 0.2 M) were added to solid **1**. Then, where applicable, the solution of the promoter was added under stirring, with the subsequent addition of alkane. For oxidation of cyclohexane, a hydrogen peroxide solution (50%, aqueous) was added dropwise within 10 seconds to a hot (50 °C) solution of the other components. For oxidation of *cis*-1,2-dimethylcyclohexane (*cis*-1,2-DMCH), a solid oxidant, *m*-chloroperoxybenzoic acid (*m*-CPBA), was dissolved in CH_3CN (typically 30 mg in 1 mL of CH_3CN) and added dropwise in the same way as H_2O_2. (CAUTION: the combination of H_2O_2 or *m*-CPBA with organic compounds at elevated temperatures may be explosive!) In all cases the final reaction volume was 5 mL. Samples were quenched at room temperature with an excess of solid PPh_3 and directly analysed by GC and GC-MS techniques.

Catalytic amidation of cyclohexane

The reactions were typically carried out under an N_2 atmosphere in a thermostated Schlenk tube under vigorous stirring. Firstly the catalyst was introduced into the tube in the solid form. Then benzene (1 mL) and cyclohexane (0.54 mL) were added in this order. The oxidant ($^tBuOO^tBu$, 184 μL) was then added at room temperature and the mixture was immediately frozen with liquid nitrogen. The atmosphere was pumped and filled with N_2 a few times in order to remove air. The frozen mixture was left to warm up under vacuum (to degasify) until becoming liquid and the above procedure was repeated. Finally the Schlenk tube was filled with N_2 and the reaction mixture was heated at 90 °C for 24 h. Then the reaction mixture was cooled to room temperature and 10 mL of CH_3CN and 100 μL of α,α,α-trifluorotoluene (GC standard) were added. The resulting mixture was directly analysed by GC/GC-MS techniques.

Results and discussion

Synthesis and spectroscopic analysis

Compounds **1** and **2** were formed through the self-assembly reactions of copper powder, iron(II) or manganese(II) chloride, pivalic acid (HPiv) and *N*-*tert*-butyldiethanolamine (H_2tBuDea) in acetonitrile solution in the presence of triethylamine, using the molar synthetic ratio of $Cu : FeCl_2/MnCl_2 : HPiv : H_2t$BuDea = 1 : 2 : 1 : 6. Such a ratio was chosen on the basis of our previous experience[2] and also to prevent the formation of very stable $\{Cu_2(Piv)_4\}$ dimers. The reactions were brought to completion by heating and stirring until the total dissolution of copper was observed (2 h for **1** and 5 h for **2**). Dark-brown microcrystals of **1** were formed within four days after standing of the resulting solution at r.t. In the case of **2**, no product formation was observed after one month standing of the resulting dark-brown solution at r.t. To promote crystallization, ^{i}PrOH was added in small portions to this solution the next month. A small amount of dark-brown crystals, suitable for X-ray crystallographic study, was formed, but they were incorporated into the simultaneously formed dark-brown oil. The crystals were carefully removed from the oil, washed with methanol and dried. A synthetic procedure was repeated a few times aiming to improve the yield of the product and trying to avoid the formation of the oily substance, but all of them were unsuccessful. We can assume that in the case of **2**, the heterometallic compound could not be isolated from the initial acetonitrile solution without the addition of ^{i}PrOH probably due to the high solubility of the complex in this solvent. But, at the same time, such addition, apart from leading to the crystal formation, also led to the undesirable oil.

The general reaction can be written as follows (M = Fe (**1**), Mn (**2**); n = 0 (**2**); 0.5 (**1**)):

$$4Cu^0 + 2(M^{II}Cl_2 \cdot 4H_2O) + 4HPiv + 4H_2tBuDea + 3Et_3N + 2.5O_2 + nCH_3CN \rightarrow [Cu^{II}_4M^{III}_2(OH)(Piv)_4(tBuDea)_4Cl] \cdot nCH_3CN + 3Et_3N \cdot HCl + 12H_2O$$

The IR spectra of complexes **1** and **2** are similar. The broad band in the 3300–3500 cm^{-1} region is attributed to the ν(OH) frequencies. In both cases, the very strong bands near 1550 cm^{-1} and 1420 cm^{-1} are assigned to the antisymmetric and symmetric COO^- stretching frequencies of pivalate, respectively. The difference in wavenumbers between these values, Δ = 130 cm^{-1}, indicates the existence of bridging carboxylate ligands[16] in the structures of the compounds, which is in line with the X-ray structure determination.

The phase purity of the bulk sample of **1** was confirmed by powder X-ray analysis (Fig. S1†).

Crystal structures

The single crystal X-ray analysis reveals that both $[Cu_4Fe_2(OH)(Piv)_4(tBuDea)_4Cl]\cdot 0.5CH_3CN$ (**1**) and $[Cu_4Mn_2(OH)(Piv)_4(tBuDea)_4Cl]$ (**2**) (Fig. 1 and S2†) are based on a hexanuclear $\{Cu_4M_2(\mu\text{-}O)_7(\mu_3\text{-}O)_2\}$ (where M = Fe, Mn) core (Fig. 2), which belongs to the general $\{M_6(\mu\text{-}X)_7(\mu_3\text{-}X)_2\}$ (M = metal atom, X = bridging atom) molecular structure type obtained by the exclusion of all non-bridging non-metal atoms.

In the crystal structures all pivalate and *N-tert*-butyldiethanolamine ligands are completely deprotonated and show bidentate (O,O) and tridentate (O,N,O) coordination, respectively, thus accounting for the molecular structure type formation and for the metal ion charge compensation. Both crystal structures have the crystallographically independent copper(II) metal atoms, Cu1, Cu3 and Cu4, which are five coordinated and have NO_4 donor sets. The Cu–O(N) bonds in **1** and **2** lie in the range from 1.877(2) to 2.438(10) Å (Table S1†), while the O–Cu–O(N) bond angles vary from 77.9(3) to 174.1(3)°. In contrast, the Cu2 atom, in both **1** and **2** (for **2** with 68% because of the disorder of Cl1 atom), is six coordinated and has a NO_4Cl donor environment formed by the nitrogen and oxygen atoms of the organic ligands [Cu2–O(N) = 1.935(8)–2.615(3) Å, Table S1†] and the chloride atom [Cu2–Cl1 = 2.2548(11) and Cu2–Cl1B = 2.194(9) Å, for **1** and **2**, respectively]. Due to the disorder, in the case of **2**, the five coordinated Cu2 atom is also observed with 32% probability. Each of the crystallographically independent Fe(III) atoms in **1**, Fe1 and Fe2, adopts a distorted octahedral geometry with the Fe–O distances varying from 1.924(2) to 2.105(2) Å. The *cis* and *trans* O–Fe–O bond angles range from 85.01(10) to 96.16(10)° and from 171.48(10) to 178.73(10)°, respectively (Table S1†). Similar to **1**, both Mn1 and Mn2 in **2** are crystallographically independent and show distorted octahedral environments with the Mn–O bonds in the range of 1.854(7)–2.296(7) Å and with *cis* and *trans* O–Mn–O angles in the ranges of 82.7(3)–97.6(3)° and 171.4(3)–178.3(3)°, respectively (Table S1†). One of the interesting features of both crystal structures is the hydroxido bridge between the iron(III) or manganese(III) atoms with the angle M1–O23–M2 equal to 140.15(12) and 140.5(5)°, for **1** and **2**, respectively. Within the hexanuclear molecules of **1** and **2** the nearest (M–O–M) Cu···Cu distances vary from 2.94 to 3.22 Å, the nearest Cu···M (M = Fe, Mn) ones range from 2.99 to 3.46 Å and the Fe···Fe and Mn···Mn separations are 3.78 and 3.89 Å, for **1** and **2**, respectively. For both structures, the bulky *N-tert*-butyl groups in the organic ligands prevent the formation of coordination or hydrogen bonds between adjacent hexanuclear molecules with a further increase of the dimensionality of the final architecture (Fig. 3 and 4). In contrast to the crystal lattice of **2**, in the structure of **1**, acetonitrile solvent molecules are located in the cavities between neighbouring hexanuclear molecules (Fig. 3).

The analysis of the Molecular Structure Type (MST)[2,17] $\{M_6(\mu\text{-}X)_7(\mu_3\text{-}X)_2\}$ of **1** and **2** (Fig. 2) reveals that it can be represented as a combination of two $M_3(\mu\text{-}X)_2(\mu_3\text{-}X)$ fragments joined together by three bridging oxygen atoms (see the detailed discussion and Tables S2 and S3 in the ESI†).

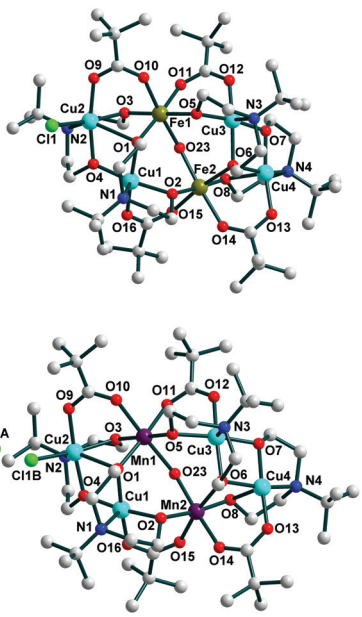

Fig. 1 Molecular structures of **1** (top) and **2** (bottom) in the ball-and-stick representation with atom numbering. The hydrogen atoms are omitted for clarity.

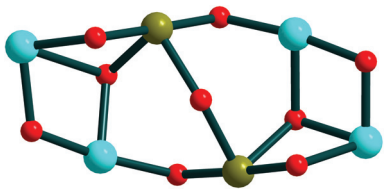

Fig. 2 The ball-and-stick representation of the hexanuclear $\{Cu_4M_2(\mu\text{-}O)_7(\mu_3\text{-}O)_2\}$ (M = Fe, Mn) core showed on the example of **1**. Colour scheme: Fe, olive; Cy, cyan; O, red.

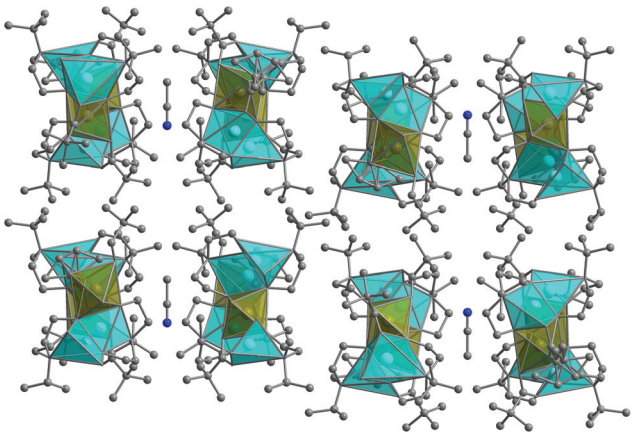

Fig. 3 Polyhedral representation of the packing of hexanuclear molecules in **1** viewed down the *a* axis. Colour scheme: Fe, olive; Cu, cyan; N, blue; C, grey.

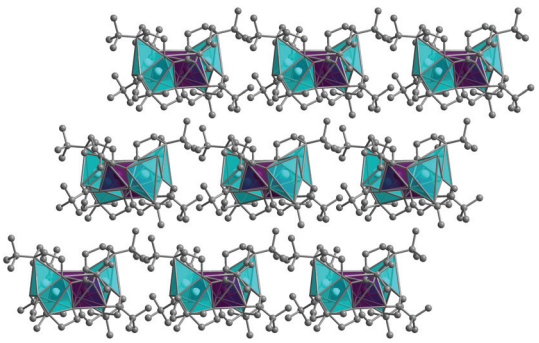

Fig. 4 Polyhedral representation of the packing of hexanuclear molecules in **2** viewed down the *b* axis. Colour scheme: Mn, dark purple; Cu, cyan; C, grey.

According to the Cambridge Structural Database (CSD, v. 5.37),[18] such a MST is rather rare. Although there are more than 1700 structures of coordination compounds containing the fragment $M_3(\mu\text{-}X)_2(\mu_3\text{-}X)$ in the CSD, only two structures were found to fit exactly this MST (CSD refcodes TALPAX and ZIHDID). Both these are polyoxometalate compounds of tungsten.[19]

ESI-MS spectrometry

The electrospray mass spectra (ESI-MS) of acetonitrile solutions of **1** were recorded to establish the structure of the compound in solution. In the negative MS mode only a noisy, low-intensity spectrum was seen. In contrast, the ESI-MS spectrum in the positive mode revealed a strong peak at 1422.99 m/z, which is close to the molecular weight of **1** (Fig. 5). The isotopic distribution fits well with that expected for the cation $[\mathbf{1}\text{–Cl–CH}_3\text{CN}]^+$. Hence, the hexanuclear core of **1** retains its integrity in solution.

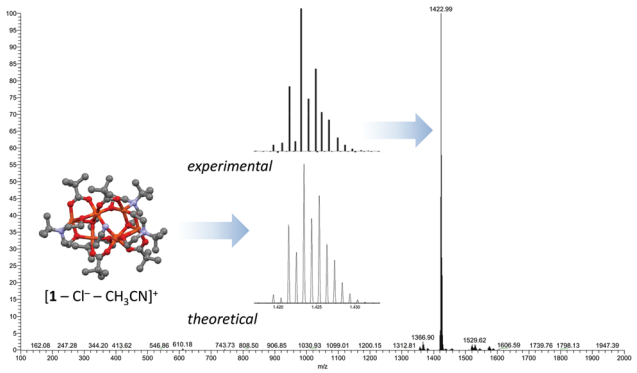

Fig. 5 ESI-MS spectrum of an acetonitrile solution of **1**, showing the peak of its molecular ion (after the elimination of chloride ligand and solvated acetonitrile).

Magnetic properties

The magnetic functions (temperature dependence of the magnetic susceptibility corrected for the underlying diamagnetism and transformed to the effective magnetic moment, and the field dependence of the magnetization per formula unit) are presented in Fig. 6. The effective magnetic moment at room temperature adopts a value of $\mu_{\text{eff}} = 7.8\mu_B$ that is much lower than the spin-only value calculated as $\mu_{\text{eff}}(\text{so})/\mu_B = g\{2{\cdot}S_{\text{Fe}}(S_{\text{Fe}} + 1) + 4{\cdot}S_{\text{Cu}}(S_{\text{Cu}} + 1)\}^{1/2} = 9.1$. On cooling it gradually decreases and at $T = 2.0$ K it is only $\mu_{\text{eff}} = 2.2\mu_B$.

This feature is typical for the exchange interaction of an antiferromagnetic nature. The magnetization per formula unit at $T = 2.0$ K and $B = 7$ T reads $M_{\text{mol}}/N_A = 1.9\mu_B$ and it lies much below the spin-only value of $M_{\text{mol}}/N_A\mu_B = 2g_{\text{Fe}}S_{\text{Fe}} + 4g_{\text{Cu}}S_{\text{Cu}} = 14$ that again is a fingerprint of the sizable antiferromagnetic coupling.

The coupling paths in complex **1** are rather complex and described at least by the three different coupling constants $J_{\text{Fe–Cu}}$, $J_{\text{Cu–Cu}}$ and $J_{\text{Fe–Fe}}$ between the adjacent centres connected by one bridging oxygen atom. The angle Fe–O–Fe = 140.2° induces a rather negative value of $J_{\text{Fe–Fe}}$. Two Cu–O–Cu angles

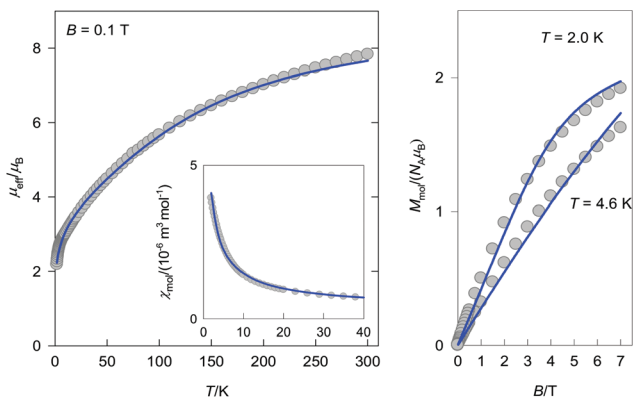

Fig. 6 Magnetic functions for **1**. Solid lines – calculated with the model of isotropic exchange.

are asymmetric (113.7° and 90.5° for one pair, and 103.6° and 93.9° for another one), which reveals that the ferromagnetic portion is fully compensated by the antiferromagnetic one yielding effectively $J_{Cu-Cu} < 0$. On the same basis also $J_{Fe-Cu} < 0$ is expected.

The spin space consists of $N = 6^2 \cdot 2^4 = 576$ functions which determine the dimension of the spin Hamiltonian matrices subjected to manifold diagonalization. The situation is much simplified when the spin symmetry is utilized which causes a factoring of the spin Hamiltonian matrices according to the spin quantum number. Then the number of spin states with $S_{min} = 0$ to $S_{max} = 7$ is 6, 14, 16, 16, 15, 11, 5 and 1. Thus $N_S = 16$ is the maximum dimension of a block for $S = 2$ and $S = 3$. However, the Zeeman term is diagonal only in the case of uniform g-factors that might be a good approximation in the present case where $g_{Cu} = 2.2$ and $g_{Fe} = 2.0$ are expected giving rise to $g_{eff} \sim 2.1$. The possible zero-field splitting is little effective in the present case.

Experimental data were fitted by exploiting an advanced genetic algorithm with the error functional that combines relative errors of the susceptibility and magnetization, *i.e.* $F = w_1 \cdot R(\chi) + (1 - w_1) \cdot R(M)$. To this end: $J_{Fe-Cu}/hc = -6.9$, $J_{Cu-Cu}/hc = -4.1$, $J_{Fe-Fe}/hc = -24.2$ (all in cm^{-1} conforming to the definition $\hat{H}_{AB} = -J(\vec{S}_A \cdot \vec{S}_B)$) and $g_{eff} = 2.00$. The minor corrections are the temperature-independent magnetism $\chi_{TIM} = -0.5 \times 10^{-9}$ m^3 mol^{-1} and the molecular-field correction $(zj)/hc = 0.31$ cm^{-1}. The agreement factors are $R(\chi) = 0.034$, $R(M) = 0.049$ and the calculated data are drawn as lines in Fig. 6. Some deviations for the magnetization under a high field are attributed to the effect of the zero-field splitting arising from the single-ion anisotropy for Fe(III) centres.

The structural data for a number of hydroxido-bridged Fe(III) complexes are compiled in Table 1 indicating that a magnetostructural correlation J *vs.* Fe–OH–Fe angle might exist. More detailed insight brought statistical multivariate methods.[20] The cluster analysis classifies the selected complexes into three groups based upon the "similarity distance" (Wards method, squared Euclidean norm) as shown in Fig. S3† – left. This assignment has been utilized in Fig. S3† – right where the J *vs.* Fe–O–Fe angle correlation is displayed. The title complex (No. 11 in Table 1) lies outside that correlation probably due to the fact that it consists of only a single Fe–OH–Fe bridge.

The principal component analysis (Fig. S4†) shows which variables correlate, anticorrelate or do not correlate: the J values anticorrelate with the Fe–(OH)–Fe bond angle. Three groups of objects are well separated. Surprisingly, the expected J (or $-J$) *vs.* P correlation (as outlined by Gorun and Lippard[21]) does not exist in the given group of complexes as proven by the Pearson correlation analysis (Table 2).

The mathematical forms of the magnetostructural J-correlations in Fe(III) polynuclear complexes are still a developing task, from early simple[21] to more sophisticated ones.[22]

Catalytic oxidation of cyclohexane with H_2O_2

The catalytic properties of complex **1** in the mild oxidation of cyclohexane were investigated (Scheme 1). Cyclohexane was selected as a recognized model substrate for C–H activation tests.[1a] Reaction of cyclohexane (0.2 M) with aq. H_2O_2 (1 M; 5 equiv.) in the presence of complex **1** (1.4×10^{-4} M; 0.07 mol%) in CH_3CN, without any promoter, afforded cyclohexanol and cyclohexanone at a very low yield of 0.6% (based on cyclo-

Table 2 Pair correlation coefficients for variables

	Fe···Fe	Fe–O–Fe	Fe–O	P	J
Fe···Fe		0.9864	0.2124	0.2339	−0.5663
Fe–O–Fe	0.9864		0.0560	0.1002	−0.6105
Fe–O	0.2124	0.0560		0.8454	0.1712
P	0.2339	0.1002	0.8454		0.1489
J	−0.5663	−0.6105	0.1712	0.1489	

Table 1 Structural data for hydroxido-bridged Fe(III) complexes

No	Refcode	Fe···Fe/Å	Fe–O–Fe/°	Fe–O1/Å	Fe–O2/Å	Fe–O_{av}/Å	P/Å	J/cm^{-1}	Bridges	Complex	Ref.
1	AVOHID	3.066	102.36	2.004	1.930	1.967	1.930	−4.2	μ-$(OH)_2$	$[Fe_2(OH)_2(L^1)_2]$	25
2	AVOHAV	3.128	100.4	2.085	1.985	2.035	1.985	−8.2	μ-$(OH)_2$	$[Fe_2(OH)_2(L^2)_2]$	26
3	ZAQFAY	3.085	100.7	2.002	2.005	2.004	2.002	−11.0	μ-$(OH)_2$	$[Fe_2(OH)_2(HL^3)_2](ClO_4)_2$	26
4	EQOFAS	3.072	100.0	2.008	2.002	2.005	2.002	−14.4	μ-$(OH)_2$	$[Fe_2(OH)_2(L^4)_2(H_2O)_4]\cdot 2H_2O$	27
5	XPYAFE	3.078	103.2	1.989	1.938	1.964	1.938	−14.6	μ-$(OH)_2$	$[Fe_2(OH)_2(H_2O)_2(OH\text{-}L^5)_2]\cdot 4H_2O$	28
6	CAWNIX	3.162	107.0	1.98	1.95	1.965	1.95	−14.8	μ-(OH) (OPh)	$[Fe_2(OH)(L^6)Cl_2]\cdot C_4H_8$	29
7	CAHJEA	3.155	102.8	2.055	1.980	2.017	1.980	−20.8	μ-$(OH)_2$	$[Fe_2(OH)_2(L^7)_2]\cdot 2H_2O\cdot 2Py$	30
8	PICAFE	3.089	103.6	1.993	1.937	1.965	1.937	−22.8	μ-$(OH)_2$	$[Fe_2(OH)_2(H_2O)_2(L^8)_2]$	28
9	HXAPFE	3.118	105.3	1.986	1.937	1.962	1.937	−23.4	μ-$(OH)_2$	$[Fe_2(OH)_2(H_2O)_2(L^9)_2]\cdot 2H_2O$	31
10	DEWPIE10	3.137	106.3	1.980	1.941	1.985	1.941	−24.0	μ-(OH) (OPh)	$[Fe_2(OH)(H_2O)_2(L^{10})]\cdot 4H_2O$	32
11	1447617[a]	3.777	140.2	2.029	1.989	2.009	1.989	−24.2	μ-(OH)	**1**	This work
12	COCJIN	3.438	123.0	1.960	1.952	1.977	1.952	−34.0	μ-(OH) $(OAc)_2$	$[Fe_2(OH)(OAc)_2(L^{11})_2]ClO_4$	33

[a] CCDC number, L^1 = 2,2′-((methylimino)bis(methylene))bis(6-*t*-butyl-4-methylphenolato), L^2 = 2,2′-((((pyridin-2-yl)methyl)imino)bis(methylene))bis(4,6-dimethylphenolato), L^3 = macrocyclic tetraaminodiphenol, H_2L^4 = 3,4-dihydroxycyclobutene-1,2-dione (squaric acid), L^5 = 4-hydroxo-2,6-pyridinedicarboxylato, L^6 = trisalicylidenetriethylenetetramine, L^7 = *N*,*N*′-ethylenebis(salicylamine), L^8 = 2,6-pyridinedicarboxylato, L^9 = 4-dimethylamino-2,6-pyridinedicarboxylato, H_5L^{10} = *N*,*N*′-(2-hydroxy-5-methyl-1,3-xylylene)bis[*N*-(carboxymethyl) glycine], L^{11} = hydrotris(1-pyrazolyl) borate. Convention: $\hat{H}_{AB} = -J(\vec{S}_A \cdot \vec{S}_B)$. P is the shortest superexchange pathway defined as the shortest distance between the metal and the bridging ligand(s).

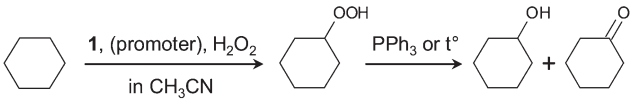

Scheme 1 Oxidation of cyclohexane with hydrogen peroxide catalysed by **1**.

hexane) after 2 h reaction time at 50 °C, with an A/K (cyclohexanol/cyclohexanone) mole ratio of 2.9 after reduction with PPh_3.[23] No further yield increase with the time was observed. The reaction rate was 1.9×10^{-7} M s^{-1}.

It is known that promoting agents (such as inorganic and carboxylic acids) are able to enhance the catalytic activity of coordination compounds in alkane oxidation.[1a] Considering the reported data for the catalytic activities of copper and iron complexes, we selected nitric, acetic, trifluoroacetic (TFA) and pyrazinecarboxylic (PCA) acids to be tested as promoters for the catalytic systems based on complex **1**. The promoting agents were used at a low concentration of 2.8×10^{-3} M. Acetic and trifluoroacetic acids revealed the yields of the products (1.1 and 0.2%, respectively, after 2 h reaction time, after addition of PPh_3) of the same level as that without using any promoter. The reaction rates were determined as 3.2×10^{-7} and 6.6×10^{-8} M s^{-1} and the chromatograms recorded before the addition of PPh_3 allowed the detection[24] of the peak of cyclohexyl hydroperoxide (Fig. S6†) as the main reaction product.

In contrast to acetic and trifluoroacetic acids, nitric and pyrazinecarboxylic ones led to a much higher activity with the maximum achieved product yield of 11.9 and 16.7%, respectively. The initial reaction rates W_0 were estimated as 3.9×10^{-6} and 4.3×10^{-5} M s^{-1} for HNO_3 and PCA promoters, respectively. The accumulations of reaction products, measured after the reduction of the samples with PPh_3, revealed a pronounced prevalence of cyclohexanol (Fig. 7) with cyclohexanol/cyclohexanol (A/K) ratios up to 63 and 41, respectively. The chromatograms recorded before the addition of PPh_3 revealed

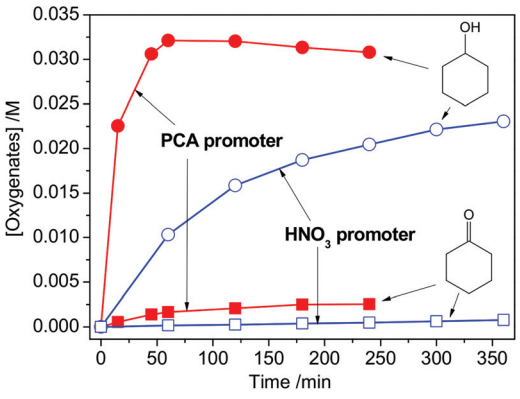

Fig. 7 Accumulations of oxygenates with the time in cyclohexane (0.2 M) oxidation with H_2O_2 (1 M, 50% aqueous), catalysed by complex **1** (1.4×10^{-4} M) in the presence of HNO_3 (2.8×10^{-3} M) and PCA (2.8×10^{-3} M), in acetonitrile at 50 °C.

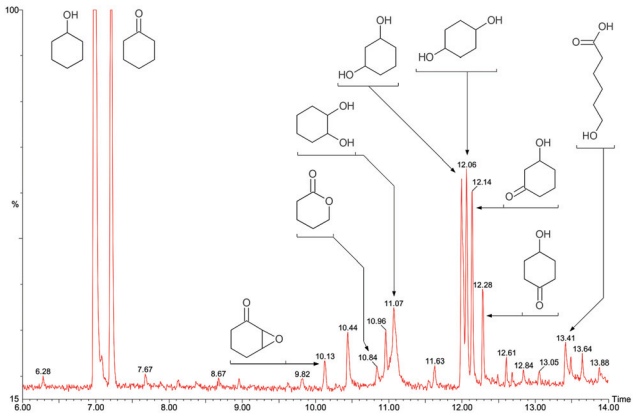

Fig. 8 Fragment of the chromatogram of the reaction (by-)products in the oxidation of cyclohexane with H_2O_2 catalysed by complex **1** in the presence of HNO_3 in acetonitrile at room temperature and 24 h reaction time.

the presence of cyclohexyl hydroperoxide as the main reaction product (Fig. S6†), as expected for the oxidation of cyclohexane with hydroxyl radicals as the main attacking species.[1a,23]

The assumption about a free radical pathway is in accord with the overoxidation pattern (Fig. 8) recorded after 24 h (for HNO_3 promoter). The products of hydroxyl radical attack at cyclohexanol, cyclohexanone and cyclohexyl hydroperoxide, such as cyclohexanodiols, hydroxycyclohexanones and other products, were observed (Fig. 8). This pattern is common[34] for catalytic systems oxidizing with hydroxyl radicals under conditions close to those used in the present case.

Polynuclear complexes of iron and copper are known to be efficient catalysts for the oxidation of alkanes with H_2O_2, mostly showing a free radical reaction mechanism with the formation of alkyl hydroperoxides as the main products.[1a,35] In such a case the maximum yield of primary products (alcohol, ketone and hydroperoxide) is limited by overoxidation, being at the *ca.* 50% level depending on the substrate.[36] For the cyclohexane substrate the best yields are shown by homo- and heterometallic polynuclear complexes of iron and copper, reaching 44%.[1a,6a,b,37] In the present case the maximum yield of 17% suggests that the catalytic system **1**/PCA/H_2O_2 has a moderate activity.

Catalytic oxidation of *cis*-1,2-dimethylcyclohexane with *m*-CPBA

Oxidation of substituted cyclohexanes (Scheme 2) provides a useful model in the tests for the regio- and/or stereoselectivity properties of C–H activating catalytic systems.[1a,38] Since the

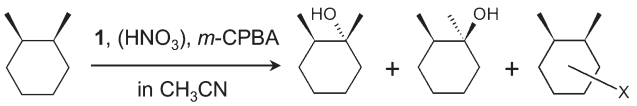

Scheme 2 Oxidation of *cis*-1,2-dimethylcyclohexane (*cis*-1,2-DMCH; X = –OH or =O) with *m*-CPBA catalysed by **1**.

hydrogen peroxide revealed a Fenton-like activity in the cyclohexane oxidation catalysed by complex **1** (see above), no stereoselectivity in the oxidation of branched substrates is expected in this case.[38c] Hence, we used a different oxidant, *m*-chloroperoxybenzoic acid (*m*-CPBA),[39] as it may afford selective oxidation of alkanes when cobalt,[40] iron,[40e,41] nickel[42] or ruthenium[43] catalysts are used. In spite of the pronounced stereoselectivity and in some cases even showing asymmetric hydroxylation,[44] the typical yield of products shown by these systems is below 15% based on the substrate.[1a]

Accumulations of the main reaction products, tertiary *cis*- and *trans*-alcohols (here and further "*cis*" and "*trans*" denote the stereoconfiguration of the methyl groups), in the course of oxidation of *cis*-1,2-dimethylcyclohexane (*cis*-1,2-DMCH; 0.1 M) with *m*-CPBA (0.027 M), catalysed by **1** (1.4×10^{-4} M) in the absence of any promoter are shown in Fig. 9, top. The initial reaction rates for *cis*- and *trans*-alcohols were determined to be nearly equal with $W_0 = 7 \times 10^{-7}$ M s^{-1}. The tertiary *cis*-alcohol, however, exhibits slightly higher final concentration, resulting in a maximum *cis*/*trans* ratio of 1.3 (Fig. 9, top, inset). Such a low *cis*/*trans* ratio corresponds to 14% of retention (see the ESI† for details of the retention index estimate) of the stereoconfiguration of the *cis*-1,2-DMCH substrate. Also, rather low 3°:2° normalized bond selectivities ranging from 4.6:1 to 6.7:1 are observed in the oxidation of *cis*-1,2-DMCH. The overall yields of the products did not exceed 2% based on the substrate and 7.4% based on the oxidant. Hence, complex **1**, in the absence of promoters, exhibits only a weak activity with the *m*-CPBA oxidant.

Chlorobenzene is a common by-product in the reactions where *m*-CPBA is used as an oxidant.[45] The formation of chlorobenzene accounts for the presence of a *m*-chlorobenzoyl radical, which undergoes decarboxylation.[45] The following hydrogen abstraction affords chlorobenzene. In the case of **1**, chlorobenzene was observed in quantities up to 4.6% of yield based on *m*-CPBA (Fig. 9, middle).

The same test performed employing nitric acid as the promoter with $[HNO_3]_0 = 5.5 \times 10^{-3}$ M (other conditions are as in Fig. 9 caption) resulted in initial reaction rates W_0 of 3.9×10^{-7} and 1.6×10^{-7} M s^{-1} for accumulations of tertiary *cis*- and *trans*-alcohols, respectively (Fig. 9, bottom). In spite of the lower reaction rates compared to those for the tests without the HNO_3 promoter (Fig. 9, top), the higher maximum *cis*/*trans* ratio of 5.3 was achieved (70% of retention of stereoconfiguration, see the ESI†). The amount of chlorobenzene was lower (Fig. 9, middle) in the presence of nitric acid (up to 1.9% of yield based on *m*-CPBA, compared to 4.6% for the non-HNO_3 test). The 3°:2° normalized selectivity after 5 h reaction time was 7.6:1, being higher than that for the test performed in the absence of nitric acid, 4.6:1. With three times higher concentration of the catalyst, 4.1×10^{-4} M, and in the presence of HNO_3, the 3°:2° normalized selectivity of 4.3:1 and the *cis*/*trans* ratio up to 2.0 were estimated (Fig. S7†).

We performed the test with the HNO_3 promoter and $[\mathbf{1}]_0 = 1.4 \times 10^{-4}$ M in the presence of 1 M of $H_2{}^{18}O$, as is known that the incorporation of oxygen from water may account for the presence of high-valent metal-oxo species.[46] It was found that the incorporation of ^{18}O into the tertiary *cis*-alcohol is at 2% level (Fig. 10, inset). However, the intensity of the 130 *m*/*z* signal (molecular ion of the ^{18}O labeled species) in the mass spectra of *trans*-alcohols was not sufficiently strong for a reliable determination of the ^{18}O incorporation level (Fig. S8†). Although the incorporation of ^{18}O into the alkane hydroxylation products (alcohols) has been undoubtedly detected, its level (up to 2%) is too weak for a definite conclusion about the

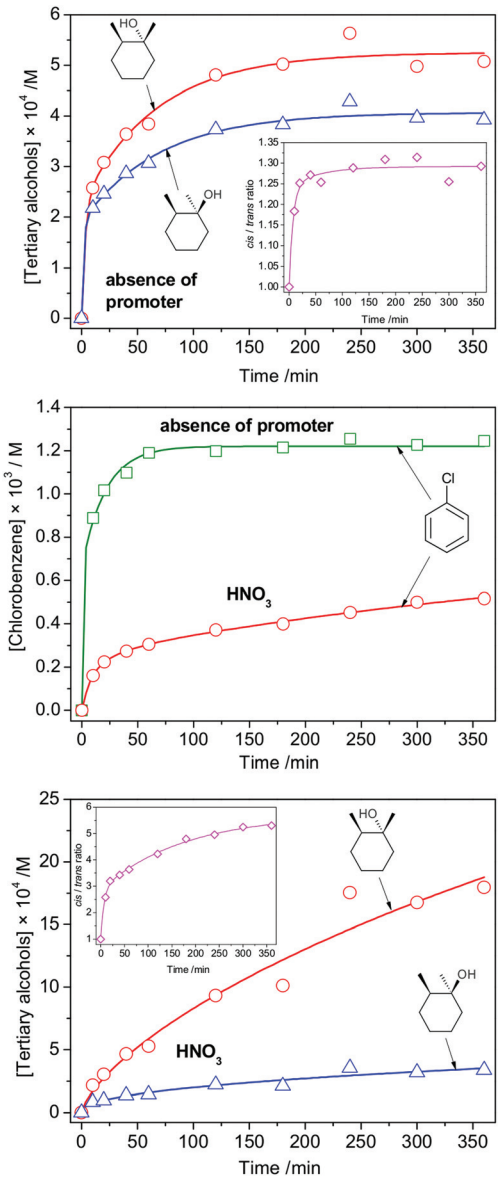

Fig. 9 Top and bottom: accumulations of the main products (tertiary *cis*- and *trans*-alcohols) in the course of *cis*-1,2-DMCH oxidation (0.1 M) with *m*-CPBA (0.027 M) catalysed by complex **1** (1.4×10^{-4} M) in the absence (top) or presence (bottom) of HNO_3 (5.5×10^{-3} M) in acetonitrile at 50 °C. The insets show the dependences of *cis*/*trans* ratios (ratios of tertiary *cis*- and *trans*-alcohols) with the time. Middle: accumulations of chlorobenzene in the absence or presence of the HNO_3 promoter.

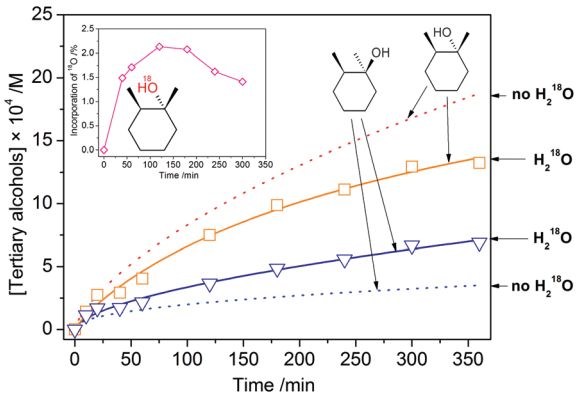

Fig. 10 Accumulations of the main products (tertiary *cis*- and *trans*-alcohols) in the course of *cis*-1,2-DMCH oxidation with *m*-CPBA catalysed by complex **1**, in the presence of the HNO_3 promoter and in the presence (symbols and solid lines) or absence (dashed lines, for comparative purpose) of $H_2{}^{18}O$ (1 M). The inset shows the incorporation of ^{18}O into the tertiary *cis*-alcohol.

nature of the C–H attacking species. Moreover, the presence of 1 M H_2O caused kinetic changes in comparison with the water-free test (Fig. 10): the maximum reached *cis*/*trans* value is 2.0 (in contrast to 5.3 in the absence of water). The changes are not likely to be from the $^{16}O/^{18}O$ kinetic isotope effect (KIE) since only a weak incorporation of ^{18}O is observed and the presence of ^{18}O causes the increase of the *trans*-product amount (Fig. 10). Moreover, the $^{16}O/^{18}O$ KIE has low typical values of 1.005–1.02,[47] only reaching higher values (1.3) in exceptional cases.[48] Similar ^{18}O incorporation levels were observed for homo- and heterometallic complexes of cobalt and cadmium with an aminoalcohol Schiff base ligand, where the oxidation of cyclohexane with *m*-CPBA afforded up to 4% of labeled alcohol.[40a] In this case the yield of products in the oxidation of *cis*-1,2-DMCH was up to 14% based on the substrate.

The chromatograms of the samples with $H_2{}^{18}O$ taken at 1 and 5 h reaction time were recorded twice, before and after the addition of PPh_3. While at 5 h time no significant differences were observed (Fig. S9†), the chromatogram at 1 h time (before the addition of PPh_3) revealed lowered amounts of tertiary *trans*-alcohol and secondary alcohols. The strong peak of chlorobenzene, observed before PPh_3 addition at 1 h (Fig. S9†), may account for the decomposition of non-reacted *m*-CPBA in the hot (200 °C) GC injector. No peaks which could be assigned to tertiary alkyl hydroperoxides have been detected, in contrast to the observation of cyclohexyl hydroperoxide in the case of oxidation of cyclohexane with the H_2O_2 oxidant (Fig. S6†). However, the absence of such peaks cannot serve as sufficient evidence for the absence of tertiary alkyl hydroperoxides. The ^{18}O enrichment levels in the sample injected prior and after the addition of PPh_3, at 5 h time, were nearly equal.

The mass spectra of the by-products, secondary alcohols as well as the respective ketones, were studied for the purpose of determination of their $^{16}O/^{18}O$ composition. The reliable estimate of the incorporation of ^{18}O into the secondary alcohols (**X**, **XI** and **XIII**, Fig. S10†) was not successful due to their strong fragmentation upon electron impact and the absence of molecular ion peaks in the respective mass spectra (although the 43 → 45 *m*/*z* shift can be observed, Fig. S11†). 2,3- and 3,4-dimethylcyclohexanones (**IX** and **XII**) were found to contain more than half of ^{18}O. This result is not surprising as ketones can exchange oxygen with water *via* a non-catalytic pathway.[34b,c,49] The strong peak of the 2,7-octanedione (**XV**) by-product (Fig. S10†), resulting from the C–C cleavage of the C_6 ring of the *cis*-1,2-DMCH substrate, was found to be labeled in the 4 : 34 : 62 ratio, corresponding to $^{16}O^{16}O : {}^{16}O^{18}O : {}^{18}O^{18}O$ compositions, respectively. The peak of 2-octanone (**VI**) contained 48% of ^{18}O. The comparison of mass spectra made in the absence and in the presence of $H_2{}^{18}O$ allowed the detection of pronounced +2 *m*/*z* shifts in the peaks of the mass spectra of **I**, **III**, **VIII**, **XIV** and **XVI** (Fig. S11†). The mass spectrum of the peak at 6.99 min (**IV**) exhibits a 126 *m*/*z* signal, appearing as a ketone derivative of *cis*-1,2-DMCH. However, the absence of +2 *m*/*z* shifts evidences against such an assignment. All the mass spectra of the (by-)products **I–XVI** are depicted in Fig. S11.†

Catalytic amidation of cyclohexane with benzamide in the presence of DTBP

Amide –NH–C(=O)– is a widespread fragment in natural and synthetic compounds.[50] Among the methods for the formation of amides, those *via* amide functionalization of aliphatic carbon to form R_3C–NH–C(=O)– are still rare.[12c,50a] Coordination compound **1** contains ligands having aliphatic *tert*-butyl groups, thus making complex **1** soluble in non-polar solvents, such as benzene. Taking this opportunity we tested the catalytic activity of **1** in the reaction of radical amidation of cyclohexane with benzamide (Scheme 3).

Oxidative amidation of cyclohexane (2.9 M) with benzamide (0.3 M) in the presence of di-*tert*-butyl peroxide, $^tBuOO^tBu$ (0.6 M) and complex **1** (6×10^{-3} M) affords *N*-cyclohexyl benzamide (peak at 12.95 min, Fig. S12†) as the main reaction product. The conversion of benzamide was lower than 5% after 24 h, at 90 °C, disclosing a low catalytic activity of **1** under the conditions studied. Such a conversion level indicates that although complex **1** is well soluble in the reaction medium, it acts as a catalyst to a limited extent. A possible explanation could be the too high steric hindrance of the *t*Bu groups of the ligands. As far as we are aware, no polynuclear complexes have been reported yet to catalyse such reactions, while from mononuclear ones the most active are those of copper with substi-

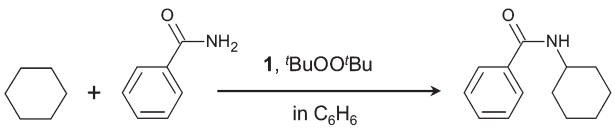

Scheme 3 Oxidative amidation of cyclohexane with benzamide catalysed by **1**.

tuted bipyridine ligands, showing almost quantitative yields.[12c,51]

The main reaction mechanism is assumed to proceed *via* the formation of free alkyl radicals, as suggested earlier for these types of reactions and copper catalysts.[12c,52] This assumption is in accord with the by-products, typical for the reactions of cyclohexyl radicals with chloro radicals[24c] and with benzene radicals,[53] according to the detection of chlorocyclohexane and phenylcyclohexane, respectively.

The formation of toluene and *N*-methylbenzamide accounts for methyl radicals which are known to appear during the thermal decomposition of ^{t}BuOO^{t}Bu.[12c] A small peak of cyclohex-2-en-1-yl benzoate (at 11.2 min, Fig. S12†) also suggests a free-radical process, as such a product is known to appear during the radical oxidation of cyclohexane with organic peroxides, including ^{t}BuOO^{t}Bu.[52] The weak peak of pivalic acid (at 4.37 min) should come from complex **1** where it serves as a ligand.

Conclusions

We have described the synthesis and crystal structures of the new heterometallic compounds $[Cu_4Fe_2(OH)(Piv)_4(t\text{BuDea})_4Cl]\cdot 0.5CH_3CN$ (**1**) and $[Cu_4Mn_2(OH)(Piv)_4(t\text{BuDea})_4Cl]$ (**2**). These complexes were prepared *via* a facile process, a one-pot open-air reaction using zerovalent copper and iron or manganese chloride as starting metal sources. Under the applied reaction conditions, *N-tert*-butyldiethanolamine and pivalic acid, having a bulky aliphatic substituent, support the formation of complexes with a high nuclear discrete structures, preventing the fusing into a coordination polymer. The obtained hexanuclear compounds show an extremely rare type of molecular core, $\{M_6(\mu\text{-}X)_7(\mu_3\text{-}X)_2\}$, where two $M_3(\mu\text{-}X)_2(\mu_3\text{-}X)$ fragments are connected by three non-metal bridges, and, as far as we are aware, **1** and **2** represent the first examples of heterometallic complexes bearing it. The analysis *via* the Cambridge Structural Database of hexanuclear structures with MSTs based on the fragment $M_3(\mu\text{-}X)_2(\mu_3\text{-}X)$ allows one to classify their main features.

For **1**, the magnetic and catalytic studies were performed. The magnetic investigation shows an antiferromagnetic coupling between the paramagnetic centres. Catalytic investigations disclosed that the activity of **1** in the oxidation of cyclohexane with H_2O_2 can be efficiently promoted with PCA (pyrazinecarboxylic acid), while the other tested acid promoters were less active or even inactive.

From the direct detection of the cyclohexyl hydroperoxide in the oxidation of cyclohexane with H_2O_2 it may be assumed that the hydroxyl radical attacks the C–H bond. In contrast, no hydroperoxides were detected when *m*-CPBA (*m*-chloroperbenzoic acid) was used as an oxidant. With the *cis*-1,2-dimethylcyclohexane substrate a moderate stereoselectivity was observed with *ca.* 2% of incorporation of ^{18}O from $H_2{}^{18}O$. The pronounced solubility of **1** in non-polar solvents allowed us to perform the test for catalytic amidation of cyclohexane with benzamide in cyclohexane/benzene medium in the presence of di-*tert*-butylperoxide. *N*-Cyclohexyl benzamide was formed as the main reaction product, presumably *via* a radical attack of cyclohexane, as evidenced by the detection of chlorocyclohexane, phenylcyclohexane and other by-products.

Conflicts of interest

There are no conflicts to declare.

Acknowledgements

This work was supported by the Foundation for Science and Technology (FCT), Portugal (projects PTDC/QEQ-QIN/3967/2014 and UID/QUI/00100/2013; fellowship SFRH/BPD/99533/2014 (D. S. N.)), and Slovak grant agencies (APVV 16-0039, VEGA 1/0919/17 and VEGA 1/0013/18). The authors acknowledge the IST Node of the Portuguese Network of Mass Spectrometry for the ESI-MS measurements.

References

1 (*a*) D. S. Nesterov, O. V. Nesterova and A. J. L. Pombeiro, *Coord. Chem. Rev.*, 2018, **355**, 199–222; (*b*) H. Li, Z. J. Yao, D. Liu and G. X. Jin, *Coord. Chem. Rev.*, 2015, **293**, 139–157; (*c*) D. Gatteschi, M. Fittipaldi, C. Sangregorio and L. Sorace, *Angew. Chem., Int. Ed.*, 2012, **51**, 4792–4800; (*d*) G. B. Shul'pin, *Catalysts*, 2016, **6**, 50.

2 D. S. Nesterov, O. V. Nesterova, V. N. Kokozay and A. J. L. Pombeiro, *Eur. J. Inorg. Chem.*, 2014, 4496–4517.

3 (*a*) C. Papatriantafyllopoulou, E. E. Moushi, G. Christou and A. J. Tasiopoulos, *Chem. Soc. Rev.*, 2016, **45**, 1597–1628; (*b*) K. Liu, W. Shi and P. Cheng, *Coord. Chem. Rev.*, 2015, **289**, 74–122; (*c*) E. J. L. McInnes, G. A. Timco, G. F. S. Whitehead and R. E. P. Winpenny, *Angew. Chem., Int. Ed.*, 2015, **54**, 14244–14269.

4 P. Buchwalter, J. Rose and P. Braunstein, *Chem. Rev.*, 2015, **115**, 28–126.

5 J. W. Sharples and D. Collison, *Coord. Chem. Rev.*, 2014, **260**, 1–20.

6 (*a*) O. V. Nesterova, E. N. Chygorin, V. N. Kokozay, V. V. Bon, I. V. Omelchenko, O. V. Shishkin, J. Titis, R. Boca, A. J. L. Pombeiro and A. Ozarowski, *Dalton Trans.*, 2013, **42**, 16909–16919; (*b*) D. S. Nesterov, E. N. Chygorin, V. N. Kokozay, V. V. Bon, R. Boca, Y. N. Kozlov, L. S. Shul'pina, J. Jezierska, A. Ozarowski, A. J. L. Pombeiro and G. B. Shul'pin, *Inorg. Chem.*, 2012, **51**, 9110–9122; (*c*) D. S. Nesterov, V. N. Kokozay, J. Jezierska, O. V. Pavlyuk, R. Boca and A. J. L. Pombeiro, *Inorg. Chem.*, 2011, **50**, 4401–4411; (*d*) D. S. Nesterov, V. N. Kokozay, V. V. Dyakonenko, O. V. Shishkin, J. Jezierska, A. Ozarowski, A. M. Kirillov, M. N. Kopylovich and A. J. L. Pombeiro, *Chem. Commun.*, 2006, 4605–4607.

7 (*a*) D. S. Nesterov, J. Jezierska, O. V. Nesterova, A. J. L. Pombeiro and A. Ozarowski, *Chem. Commun.*, 2014, **50**, 3431–3434; (*b*) D. S. Nesterov, E. C. B. A. Alegria and J. Jezierska, *Inorg. Chim. Acta*, 2017, **460**, 83–88; (*c*) E. N. Chygorin, V. N. Kokozay, I. V. Omelchenko, O. V. Shishkin, J. Titis, R. Boca and D. S. Nesterov, *Dalton Trans.*, 2015, **44**, 10918–10922; (*d*) W. G. Wang, A. J. Zhou, W. X. Zhang, M. L. Tong, X. M. Chen, M. Nakano, C. C. Beedle and D. N. Hendrickson, *J. Am. Chem. Soc.*, 2007, **129**, 1014–1015.

8 O. V. Nesterova, M. V. Kirillova, M. F. C. Guedes da Silva, R. Boca and A. J. L. Pombeiro, *CrystEngComm*, 2014, **16**, 775–783.

9 (*a*) A. M. Ako, V. Mereacre, R. Clerac, I. J. Hewitt, Y. H. Lan, G. Buth, C. E. Anson and A. K. Powell, *Inorg. Chem.*, 2009, **48**, 6713–6723; (*b*) V. Mereacre, A. M. Ako, M. N. Akhtar, A. Lindemann, C. E. Anson and A. K. Powell, *Helv. Chim. Acta*, 2009, **92**, 2507–2524; (*c*) F. Klower, Y. H. Lan, J. Nehrkorn, O. Waldmann, C. E. Anson and A. K. Powell, *Chem. – Eur. J.*, 2009, **15**, 7413–7422.

10 (*a*) G. B. Shul'pin, *Catalysts*, 2016, **6**, 50; (*b*) E. P. Talsi, R. V. Ottenbacher and K. P. Bryliakov, *J. Organomet. Chem.*, 2015, **793**, 102–107; (*c*) W. Liu and J. T. Groves, *Acc. Chem. Res.*, 2015, **48**, 1727–1735; (*d*) K. P. Bryliakov and E. P. Talsi, *Coord. Chem. Rev.*, 2014, **276**, 73–96.

11 (*a*) J. F. Hartwig and M. A. Larsen, *ACS Cent. Sci.*, 2016, **2**, 281–292; (*b*) J. F. Hartwig, *J. Am. Chem. Soc.*, 2016, **138**, 2–24.

12 (*a*) J. P. Wan and Y. F. Jing, *Beilstein J. Org. Chem.*, 2015, **11**, 2209–2222; (*b*) H. T. Zeng and J. M. Huang, *Org. Lett.*, 2015, **17**, 4276–4279; (*c*) B. L. Tran, B. J. Li, M. Driess and J. F. Hartwig, *J. Am. Chem. Soc.*, 2014, **136**, 2555–2563; (*d*) R. T. Gephart, D. L. Huang, M. J. B. Aguila, G. Schmidt, A. Shahu and T. H. Warren, *Angew. Chem., Int. Ed.*, 2012, **51**, 6488–6492.

13 *SAINT*, Bruker AXS Inc., Madison, WI, 2004.

14 Bruker, *APEX2 & SAINT*, AXS Inc., Madison, WI, 2004.

15 G. M. Sheldrick, *Acta Crystallogr., Sect. C: Struct. Chem.*, 2015, **71**, 3–8.

16 K. Nakamoto, *Infrared and Raman Spectra of Inorganic and Coordination Compounds, Part B, Applications in Coordination, Organometallic and Bioinorganic Chemistry*, Wiley, Chichester, 5th edn, 1997.

17 V. G. Kessler, *Chem. Commun.*, 2003, 1213–1222.

18 C. R. Groom and F. H. Allen, *Angew. Chem., Int. Ed.*, 2014, **53**, 662–671.

19 (*a*) W. P. Griffith, B. C. Parkin, A. J. P. White and D. J. Williams, *J. Chem. Soc., Chem. Commun.*, 1995, 2183–2184; (*b*) M. Hashimoto, T. Iwamoto, H. Ichida and Y. Sasaki, *Polyhedron*, 1991, **10**, 649–651.

20 *Statgraphics Centurion XV, ver. 15.1.02*, StatPoint, Inc., 2006.

21 S. M. Gorun and S. J. Lippard, *Inorg. Chem.*, 1991, **30**, 1625–1630.

22 (*a*) H. Weihe and H. U. Gudel, *J. Am. Chem. Soc.*, 1997, **119**, 6539–6543; (*b*) R. Werner, S. Ostrovsky, K. Griesar and W. Haase, *Inorg. Chim. Acta*, 2001, **326**, 78–88; (*c*) K. J. Mitchell, K. A. Abboud and G. Christou, *Inorg. Chem.*, 2016, **55**, 6597–6608.

23 G. B. Shul'pin, *J. Mol. Catal. A: Chem.*, 2002, **189**, 39–66.

24 (*a*) I. Gryca, K. Czerwinska, B. Machura, A. Chrobok, L. S. Shul'pina, M. L. Kuznetsov, D. S. Nesterov, Y. N. Kozlov, A. J. L. Pombeiro, I. A. Varyan and G. B. Shul'pin, *Inorg. Chem.*, 2018, **57**, 1824–1839; (*b*) G. B. Shul'pin, D. S. Nesterov, L. S. Shul'pina and A. J. L. Pombeiro, *Inorg. Chim. Acta*, 2017, **455**, 666–676; (*c*) O. V. Nesterova, D. S. Nesterov, A. Krogul-Sobczak, M. F. C. Guedes da Silva and A. J. L. Pombeiro, *J. Mol. Catal. A: Chem.*, 2017, **426**, 506–515.

25 T. Weyhermuller, R. Wagner and P. Chaudhuri, *Eur. J. Inorg. Chem.*, 2011, 2547–2557.

26 K. K. Nanda, S. K. Dutta, S. Baitalik, K. Venkatsubramanian and K. Nag, *J. Chem. Soc., Dalton Trans.*, 1995, 1239–1244.

27 J. Carranza, J. Sletten, F. Lloret and M. Julve, *Inorg. Chim. Acta*, 2011, **371**, 13–19.

28 J. A. Thich, C. C. Ou, D. Powers, B. Vasiliou, D. Mastropaolo, J. A. Potenza and H. J. Schugar, *J. Am. Chem. Soc.*, 1976, **98**, 1425–1433.

29 B. Chiari, O. Piovesana, T. Tarantelli and P. F. Zanazzi, *Inorg. Chem.*, 1983, **22**, 2781–2784.

30 L. Borer, L. Thalken, C. Ceccarelli, M. Glick, J. H. Zhang and W. M. Reiff, *Inorg. Chem.*, 1983, **22**, 1719–1725.

31 C. C. Ou, R. A. Lalancette, J. A. Potenza and H. J. Schugar, *J. Am. Chem. Soc.*, 1978, **100**, 2053–2057.

32 B. P. Murch, F. C. Bradley, P. D. Boyle, V. Papaefthymiou and L. Que, *J. Am. Chem. Soc.*, 1987, **109**, 7993–8003.

33 W. H. Armstrong and S. J. Lippard, *J. Am. Chem. Soc.*, 1984, **106**, 4632–4633.

34 (*a*) D. S. Nesterov, O. V. Nesterova, M. F. C. Guedes da Silva and A. J. L. Pombeiro, *Catal. Sci. Technol.*, 2015, **5**, 1801–1812; (*b*) A. N. Bilyachenko, M. M. Levitsky, A. I. Yalymov, A. A. Korlyukov, A. V. Vologzhanina, Y. N. Kozlov, L. S. Shul'pina, D. S. Nesterov, A. J. L. Pombeiro, F. Lamaty, X. Bantreil, A. Fetre, D. Y. Liu, J. Martinez, J. Long, J. Larionova, Y. Guari, A. L. Trigub, Y. V. Zubavichus, I. E. Golub, O. A. Filippov, E. S. Shubina and G. B. Shul'pin, *RSC Adv.*, 2016, **6**, 48165–48180; (*c*) M. M. Vinogradov, Y. N. Kozlov, A. N. Bilyachenko, D. S. Nesterov, L. S. Shul'pina, Y. V. Zubavichus, A. J. L. Pombeiro, M. M. Levitsky, A. I. Yalymov and G. B. Shul'pin, *New J. Chem.*, 2015, **39**, 187–199; (*d*) M. M. Vinogradov, Y. N. Kozlov, D. S. Nesterov, L. S. Shul'pina, A. J. L. Pombeiro and G. B. Shul'pin, *Catal. Sci. Technol.*, 2014, **4**, 3214–3226.

35 G. B. Shul'pin, *Dalton Trans.*, 2013, **42**, 12794–12818.

36 G. B. Shul'pin, Y. N. Kozlov, L. S. Shul'pina, A. RKudinov and D. Mandelli, *Inorg. Chem.*, 2009, **48**, 10480–10482.

37 (*a*) A. N. Bilyachenko, M. M. Levitsky, A. I. Yalymov, A. A. Korlyukov, V. N. Khrustalev, A. V. Vologzhanina, L. S. Shul'pina, N. S. Ikonnikov, A. E. Trigub, P. V. Dorovatovskii, X. Bantreil, F. Lamaty, J. Long, J. Larionova, I. E. Golub, E. S. Shubina and G. B. Shul'pin, *Angew. Chem., Int. Ed.*, 2016, **55**, 15360–15363;

(*b*) M. V. Kirillova, Y. N. Kozlov, L. S. Shul'pina, O. Y. Lyakin, A. M. Kirillov, E. P. Talsi, A. J. L. Pombeiro and G. B. Shul'pin, *J. Catal.*, 2009, **268**, 26–38; (*c*) A. M. Kirillov, M. N. Kopylovich, M. V. Kirillova, M. Haukka, M. F. C. Guedes da Silva and A. J. L. Pombeiro, *Angew. Chem., Int. Ed.*, 2005, **44**, 4345–4349.

38 (*a*) J. Serrano-Plana, W. N. Oloo, L. Acosta-Rueda, K. K. Meier, B. Verdejo, E. Garcia-Espana, M. G. Basallote, E. Munck, L. Que, A. Company and M. Costas, *J. Am. Chem. Soc.*, 2015, **137**, 15833–15842; (*b*) D. Font, M. Canta, M. Milan, O. Cusso, X. Ribas, R. J. M. Klein Gebbink and M. Costas, *Angew. Chem., Int. Ed.*, 2016, **55**, 5776–5779; (*c*) G. Olivo, O. Lanzalunga and S. Di Stefano, *Adv. Synth. Catal.*, 2016, **358**, 843–863.

39 H. Hussain, A. Al-Harrasi, I. R. Green, I. Ahmed, G. Abbas and N. U. Rehman, *RSC Adv.*, 2014, **4**, 12882–12917.

40 (*a*) O. V. Nesterova, K. V. Kasyanova, V. G. Makhankova, V. N. Kokozay, O. Y. Vassilyeva, B. W. Skelton, D. S. Nesterov and A. J. L. Pombeiro, *Appl. Catal., A*, 2018, **560**, 171–184; (*b*) O. V. Nesterova, M. N. Kopylovich and D. S. Nesterov, *RSC Adv.*, 2016, **6**, 93756–93767; (*c*) G. B. Shul'pin, D. A. Loginov, L. S. Shul'pina, N. S. Ikonnikov, V. O. Idrisov, M. M. Vinogradov, S. N. Osipov, Y. V. Nelyubina and P. M. Tyubaeva, *Molecules*, 2016, **21**, 1593; (*d*) J. Nakazawa, A. Yata, T. Hori, T. D. P. Stack, Y. Naruta and S. Hikichi, *Chem. Lett.*, 2013, **42**, 1197–1199; (*e*) W. Nam, J. Y. Ryu, I. Kim and C. Kim, *Tetrahedron Lett.*, 2002, **43**, 5487–5490; (*f*) W. Nam, I. Kim, Y. Kim and C. Kim, *Chem. Commun.*, 2001, 1262–1263.

41 (*a*) W. Nam, M. H. Lim, S. K. Moon and C. Kim, *J. Am. Chem. Soc.*, 2000, **122**, 10805–10809; (*b*) M. Kodera, H. Shimakoshi and K. Kano, *Chem. Commun.*, 1996, 1737–1738; (*c*) R. Mayilmurugan, H. Stoeckli-Evans, E. Suresh and M. Palaniandavar, *Dalton Trans.*, 2009, 5101–5114.

42 (*a*) M. Balamurugan, R. Mayilmurugan, E. Suresh and M. Palaniandavar, *Dalton Trans.*, 2011, **40**, 9413–9424; (*b*) M. Sankaralingam, M. Balamurugan, M. Palaniandavar, P. Vadivelu and C. H. Suresh, *Chem. – Eur. J.*, 2014, **20**, 11346–11361; (*c*) T. Nagataki, Y. Tachi and S. Itoh, *Chem. Commun.*, 2006, 4016–4018; (*d*) T. Nagataki, K. Ishii, Y. Tachi and S. Itoh, *Dalton Trans.*, 2007, 1120–1128; (*e*) T. Corona, F. F. Pfaff, F. Acuna-Pares, A. Draksharapu, C. J. Whiteoak, V. Martin-Diaconescu, J. Lloret-Fillol, W. R. Browne, K. Ray and A. Company, *Chem. – Eur. J.*, 2015, **21**, 15029–15038.

43 T. Kojima, K. I. Hayashi, S. Y. Iizuka, F. Tani, Y. Naruta, M. Kawano, Y. Ohashi, Y. Hirai, K. Ohkubold, Y. Matsuda and S. Fukuzumi, *Chem. – Eur. J.*, 2007, **13**, 8212–8222.

44 T. Nagataki, Y. Tachi and S. Itoh, *J. Mol. Catal. A: Chem.*, 2005, **225**, 103–109.

45 A. Bravo, H. R. Bjorsvik, F. Fontana, F. Minisci and A. Serri, *J. Org. Chem.*, 1996, **61**, 9409–9416.

46 (*a*) K. A. Lee and W. Nam, *J. Am. Chem. Soc.*, 1997, **119**, 1916–1922; (*b*) W. W. Nam and J. S. Valentine, *J. Am. Chem. Soc.*, 1993, **115**, 1772–1778.

47 (*a*) S. Khan, K. R. Yang, M. Z. Ertem, V. S. Batista and G. W. Brudvig, *ACS Catal.*, 2015, **5**, 7104–7113; (*b*) J. P. Roth and C. J. Cramer, *J. Am. Chem. Soc.*, 2008, **130**, 7802–7803; (*c*) L. M. Mirica and J. P. Klinman, *Proc. Natl. Acad. Sci. U. S. A.*, 2008, **105**, 1814–1819; (*d*) L. M. Mirica, K. P. McCusker, J. W. Munos, H. W. Liu and J. P. Klinman, *J. Am. Chem. Soc.*, 2008, **130**, 8122–8123.

48 W. W. Y. Lam, W. L. Man, C. F. Leung, C. Y. Wong and T. C. Lau, *J. Am. Chem. Soc.*, 2007, **129**, 13646–13652.

49 R. V. Ottenbacher, D. G. Samsonenko, E. P. Talsi and K. P. Bryliakov, *ACS Catal.*, 2014, **4**, 1599–1606.

50 (*a*) C. Zhu, R. Wang and J. R. Falck, *Chem. – Asian J.*, 2012, **7**, 1502–1514; (*b*) J. Bariwal and E. Van der Eycken, *Chem. Soc. Rev.*, 2013, **42**, 9283–9303.

51 (*a*) Q. Michaudel, D. Thevenet and P. S. Baran, *J. Am. Chem. Soc.*, 2012, **134**, 2547–2550; (*b*) F. Teng, S. Sun, Y. Jiang, J. T. Yu and J. Cheng, *Chem. Commun.*, 2015, **51**, 5902–5905; (*c*) P. K. Chikkade, Y. Kuninobu and M. Kanai, *Chem. Sci.*, 2015, **6**, 3195–3200.

52 B. L. Tran, M. Driess and J. F. Hartwig, *J. Am. Chem. Soc.*, 2014, **136**, 17292–17301.

53 D. Liu, Y. X. Li, X. T. Qi, C. Liu, Y. Lan and A. W. Lei, *Org. Lett.*, 2015, **17**, 998–1001.

